CONCRETE LIBRARY OF JSCE NO. 24, DECEMBER 1994

EXPERIMENTAL STUDY OF THE EFFECT OF SIZE ON THE PHYSICAL PROPERTIES OF CONCRETE UNDER COMPRESSION

(Translation from Concrete Research and Technology, JCI, Vol.5, No.1, 1994)

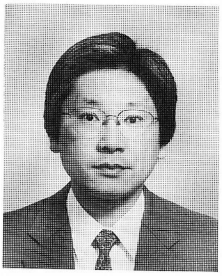
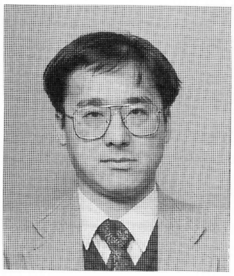
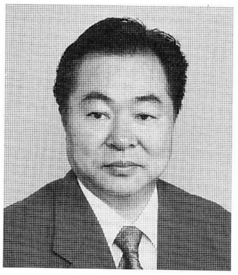
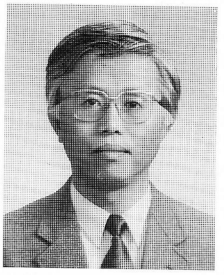

Shigemitsu HATANAKA Eiji MIZUNO Sachio KOIKE Yasuo TANIGAWA

SYNOPSIS

This paper has two main purposes: to examine the effect of specimen size on the stress-strain curves of concrete under uniaxial and triaxial compressive stress; and to understand quantitatively the cracking patterns of specimens by analyzing the size distribution data of the concrete fragments of tested specimens after failure. It is found that the effect of specimen size on the deformation behavior of concrete is greater for concrete under triaxial compression than that for concrete under uniaxial compression. In this paper, a model of compressive cracking pattern is proposed, based on an analysis of the experimental data obtained. The effect of size on the compressive deformation behavior of concrete is also discussed, highlighting the dissipation energy at cracking.

Keywords: Size effect, compression, stress-strain, cracking pattern, plastic work, fracture energy.

S.Hatanaka is an associate professor of architectural engineering at Mie University, Tsu, Japan. He received his doctorate in engineering from Nagoya University in 1984. His research interests include experimental and analytical work on the constitutive relationships of concrete materials.

E.Mizuno is an associate professor of civil engineering at Nagoya University, Nagoya, Japan. He received his doctorate in philosophy from Purdue University in 1981. His research interests include the development of constitutive relationships of engineering materials.

S.Koike is an associate professor of architectural engineering at Aichi Institute of Technology, Toyota, Japan. His research interests include experimental work on the mechanical size effect of concrete materials and reinforced concrete members.

Y.Tanigawa is a professor of architectural engineering at Nagoya University, Nagoya, Japan. He received his doctorate in engineering from Osaka University in 1974. His research interests include experimental and analytical work on the constitutive relationships of fresh and hardened concrete.

---

1. Introduction

In general, the strength and ductility of a structural member tend to decrease as the size of the member increases [1-5]. Despite this experimental fact, reduced-scale specimens are usually used in laboratory experiments, from which unconservative data tend to be obtained.

The effect of size on the compressive strength of concrete is not as great as it is on the tensile, flexural, and shearing strengths. The compressive strength of full-scale members is considered to be about 80 to 90% that of ordinary test specimens (with a cross-sectional diameter of 10 to 15 cm) [6], while some reports have pointed out that the effect of size becomes greater as the compressive strength increases [7,8]. It has also been reported that the brittleness exhibited in compressive failure tends to increase as the size of the specimen increases, and the degree of the size effect again seems to depend on the strength of the concrete [8,9].

The authors have carried out a series of experiments to investigate the effect of various factors, such as concrete strength, the magnitude and loading type of lateral pressure, and the shape of the specimen on the stress-strain relationship of normal and high-strength concrete under triaxial compression [10,11]. However, specimens used in the experiments were rather small (circular section of 10 cm in diameter and square section of 10x10 cm), compared with full-scale members. It is necessary, therefore, to discuss the effect of size in order to apply the previously obtained information to the strength and deformation analysis of full-scale members.

One of the main purposes of this paper is to examine experimentally the effect of the specimen size on the stress-strain curves of concrete under uniaxial and triaxial compressive stress. The other is to understand quantitatively the cracking pattern of specimens by analyzing of the size distribution data of concrete fragments after failure of the tested specimens.

2. Experimental procedures

2.1 Outline of experiment

An outline of experiment is shown in Table 1. Uniaxial and triaxial compression tests were conducted, using three sizes of confined concrete. Testing variables included the diameter of the specimen (D), the compressive strength of concrete (Fc), and the magnitude of the lateral confining pressure (σ_{LY}). All the specimens were cylinders with a height-diameter ratio (H/D) of unity, and the pitch (S) of the steel hoops was set at D/4.

Table 1 Outline of experiment

D (cm)	H/D	Fc (kgf/cm^2)	S	σ_{LY} (kgf/cm^2)
10	1	400	D/4	0, 25, 50
15		700		0, 50
20		1000		0, 50, 100

[Notes] D : Nominal diameter of specimen, H/D : Height-diameter ratio of specimen, Fc : Compressive strength level, S : Pitch of steel hoops, σ_{LY} : Lateral stress level at yielding of steel hoops.

The experiment can be regarded as a passive triaxial compression test, where lateral confining pressure is applied as a secondary external force to a specimen by means of surrounding steel hoops. With the passive triaxial test in particular, it is very important to distribute the confining pressure uniformly along the height of the specimen. In the experiment, therefore, specimens with H/D=1 were used, so that almost uniform dilatation along the height can be expected [10]. The estimated lateral confining pressure, calculated on the condition that all the steel hoops yield, is shown in Table 2.

2.2 Fabrication of specimens

Ordinary Portland cement, river sand (maximum size: 5mm), crushed stone (size range: 5-15mm), silica fume (only for F_c=1000 kgf/cm^2 series), superplasticizer, and steel hoops were used to make the specimens. The designed slump was 20cm and the designed compressive strengths were 400, 700, and 1000 kgf/cm^2. Specimens were capped after one day and demolded after two. The specimens were then cured in a moist room (27±1℃, relative humidity 88±2%) and tested after about 50 days. Two specimens were tested for the combination of each factor.

2.3 Loading and measurement

A load was applied to specimens with a compression testing machine (capacity: 600tf) up to the specified longitudinal strain (ε_1=20×10^{-3}). The friction at the specimen-loading platen interfaces was reduced by placing friction-reducing pads which consist of two polypropylene sheets with silicon grease between them.

To measure longitudinal strain, a pair of steel frames was attached to the specimen at the location of 0.05H (where H is the height of the specimen) from both ends of the specimen by using 4 bolts. That is, the measurement length of the longitudinal strain is constantly 0.9H. The longitudinal strain was measured with a pair of deformation transducers attached to the steel frames in the stress ascending range. In the stress descending range, the steel frames were taken away, and the strain was measured with another pair of deformation transducers that was set between loading plates. The elongation of the steel hoops was measured with a pair of wire strain gages glued to the hoops.

Table 2 Calculated lateral pressure at yielding of steel hoops

D (mm)	f_y (kgf/cm^2)	t (mm)	d (c) (mm)	σ_{LY} (kgf/cm^2)
95.2	2560	3.2	3.6 (20.2)	26.3
			7.2 (16.6)	52.6
			14.5 (9.3)	105.2
156.2	2600	4.5	6.4 (32.7)	24.7
			12.9 (26.2)	49.4
			25.7 (13.4)	98.8
204.4	3130	5.8	6.9 (44.2)	24.1
			13.9 (37.2)	48.2
			27.8 (23.3)	96.5

[Notes] D : Measured diameter of specimen (inner diameter of steel hoop), f_y : Yielding strength of steel, t : Thickness of steel hoop, d : Width of steel hoop, c : Spacing of steel hoops (S = d + c) σ_{LY} : Calculated lateral pressure at yielding of steel hoop, i.e. $\sigma_{LY} = (2 \cdot t \cdot d / S \cdot D) \times f_y$

3. Test results and discussions

3.1 Strain of hoops and lateral pressure

Figures 1(a) and (b) show examples of the variation of lateral pressure (σ_L) calculated directly from the measured strain of hoops. According to the figures and the other results of the experiment, lateral pressure is applied almost uniformly to specimens, regardless of the strength of the concrete, although the strain of the hoops tends to be large in the upper part (upper side in casting) of specimens. Therefore, the experiment can be considered to be a triaxial compressive test with passive lateral pressure.

3.2 Stress-strain curves

Figures 2(a) through (c) show the effect of specimen size on the longitudinal stress-strain curves. According to the figures, the peak stress and compressive toughness decrease markedly with increasing specimen size. A similar tendency is also observed in the other results of the experiment. Such size effects may be considered partly due to difference in the clearance (see Table 2) between hoops, in addition to the effect of size on the behavior of the concrete itself. Then, an additional test was carried out to compare stress-strain curves of specimens of Fc=700 kgf/cm² series with S=D/4 and D/8. However, no outstanding difference was observed between them.

3.3 Effect of specimen size on the peak stress

Figure 3 shows the effect of specimen size on the peak stress. The solid line is calculated from Kim's formula [12], which is identified with Blanks' test data [1]. The dashed lines indicate the upper and lower limits of the present test data, where relative strength R is expressed by the following formula:

$$R = 10/(D+a) + b \tag{1}$$

where, D: Section size of specimen (cm)
a,b: Empirical constants

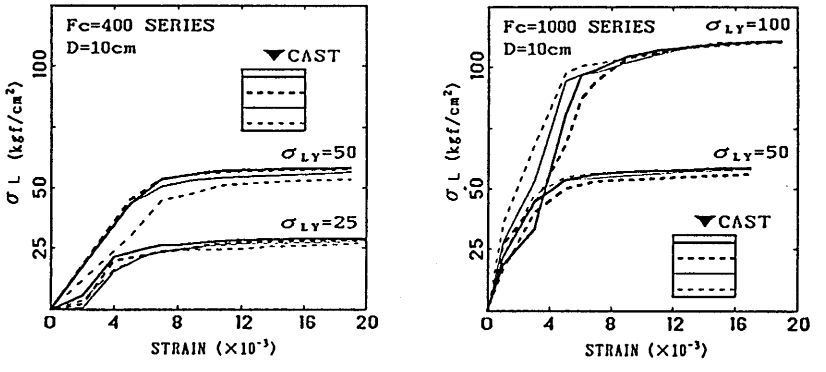

(a)Fc=400 series (b)Fc=1000 series

Fig.1 Calculated lateral pressure (σ_L) curves

Although all the test data for various conditions are plotted almost within the two lines, the effect of size on the compressive strength seems to be more remarkable for a larger confining pressure.

3.4 Concrete fragments of specimens after uniaxial compression test

Photograph 1 shows the distribution of concrete fragments after the uniaxial compression tests. In the photograph, the fragments are arranged from left to right in the order of decreasing size, the upper and lower ends of the fragments corresponding to the upper and lower ends of the specimens.

(1)Effect of concrete strength

From the surface conditions of the fragments, very rough surfaces are observed for Fc=400 kgf/cm² specimens, while surfaces are rather sharp for Fc=1000 kgf/cm² specimens. The lengths of the relatively large fragments are nearly half to one-third the original height for Fc=400 kgf/cm² specimens, while for Fc=1000 kgf/cm² specimens they are almost the same as the original heights. This is considered due to the fact that cracking occurs and propagates around the coarse aggregates for Fc=400 kgf/cm² specimens, while cracking often initiates inside or penetrates the coarse aggregates for Fc=1000 kgf/cm² specimens. The total volume of relatively small fragments (bottom right of each Photograph)

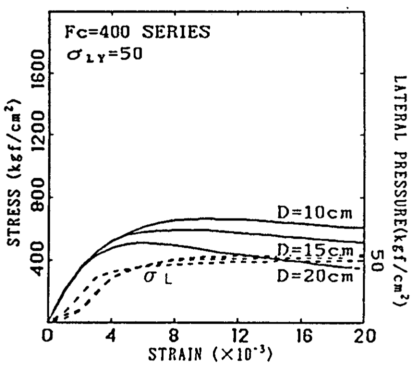

(a)Fc=400 series

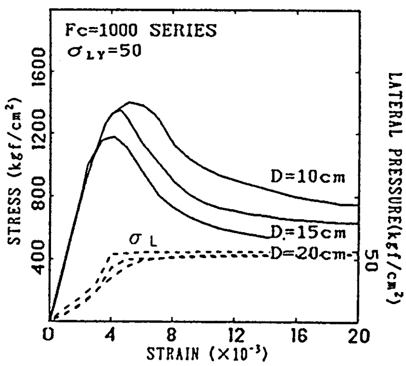

(c)Fc=1000 series

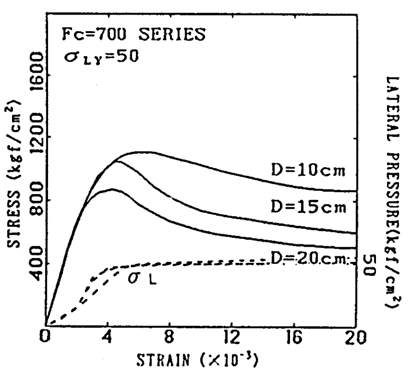

(b)Fc=700 series

Fig.2 Size effect on longitudinal stress-strain curves

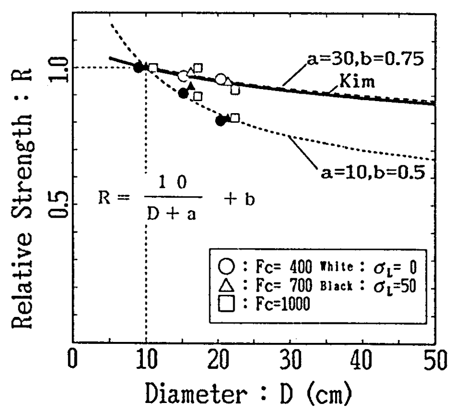

Fig.3 Size effect on peak stress

seems to decrease with increasing concrete strength, regardless of the size of the specimen.

(2) Effect of specimen size
The photographs of concrete fragments are reduced in proportion to the size ratio in order to make them all appear to have the same dimensions. Quite similar distribution patterns are observed for relatively large fragments in the photographs, independently of the size of the specimens. Namely, the actual sizes of the relatively large fragments are in proportion to the sizes of specimens.

3.5 Data-analysis for concrete fragments

The number of fragments with a volume greater than 2 cm^3 was counted and their volume was measured for σ_L=0 and 50 kgf/cm^2 specimens. In σ_L=50 kgf/cm^2 specimens, the steel hoops arranged around concrete cylinders were cut and removed from the tested specimens, then concrete cylinders were compressed axially again until they collapsed completely. The initial loading was applied up to approximately a longitudinal strain (ε) of 20×10^{-3}. Therefore, the observed cracking patterns in Photo.1 are considered those at $\varepsilon = 20 \times 10^{-3}$.

(1)Ideal cracking pattern
Figures 4(a) and (b) show the two typical cracking patterns of specimens. In cracking pattern A (Fig.4(a)), no size effect is apparent, while in pattern B (Fig.4(b)), the sizes of the fragments vary in proportion to those of specimens, which results in the most outstanding size effect. In the present study, discussion is carried out in the following, comparing the actual size distribution of fragments with these typical cracking patterns.

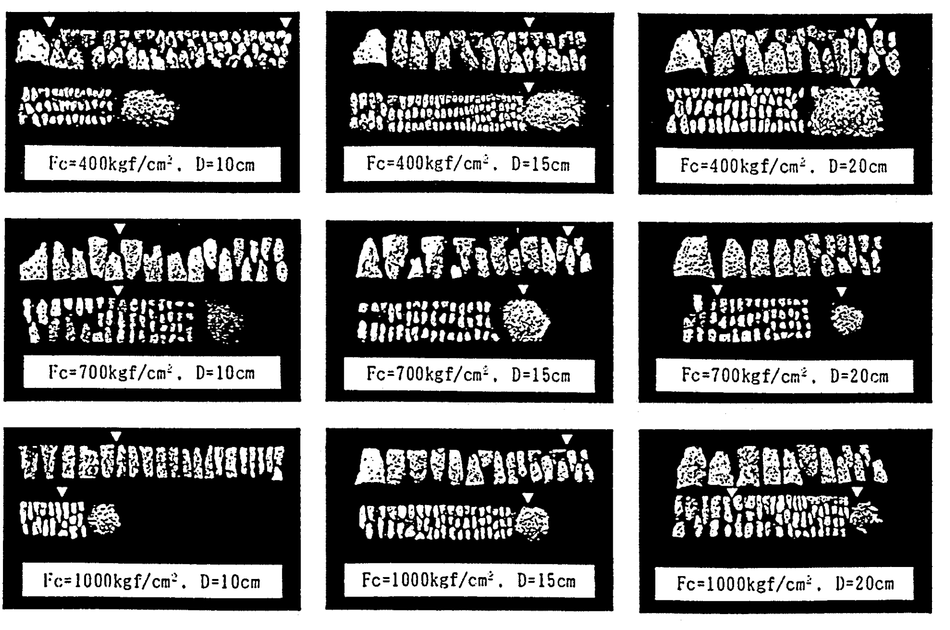

Photo.1 Concrete fragments after failure
(Uniaxial compression)

(2)Method of data-analysis

Fragments are classified into three groups, bordered by the two volumes v=2 and 36 cm^3 (see Photo.1, marked with Δ). The volume of v=2 cm^3 nearly equals to that of coarse aggregate with maximum size of diameter ϕ_a=1.5 cm, where volume $v=4\pi(\phi_a/2)^3/3 \fallingdotseq 1.8$ cm^3, provided that the aggregate is perfect sphere. The volume of v=36 cm^3, on the other hand, is the largest one, to which the fragments exist continuously at least in every 2 cm^3 interval from the volume v=2 cm^3 (see Fig.7(a)).

(3) Distribution of fragment size

Figure 5 shows the averaged occupancy ratio of large size ($v \geqq 36$ cm^3), medium size ($2 \leqq v \leqq 36$ cm^3), and small size ($v \leqq 2$ cm^3) fragments to total volume, in each size of specimen. From the present experimental data, the occupancy ratio of each range of fragment was found to be rather similar, regardless of the compressive strength Fc and lateral confining pressure σ_L.

(4) Number of medium- and large-sized fragments

i)Total number

Figure 6 shows the total numbers of medium- and large-sized fragments (above 2 cm^3). The total number N increases with increasing size of a specimen in every series, but the increasing ratio is generally not in proportion to the volume ratio of a specimen (zone A). Zones of A and B respectively correspond to the typical cracking patterns A and B in Fig.4. According to the figure, the actual patterns seem to be somewhere in-between. The total number N may be represented by the linear function of the size D of a specimen (Eq.(2) in Table 3), regardless of the lateral pressure σ_L.

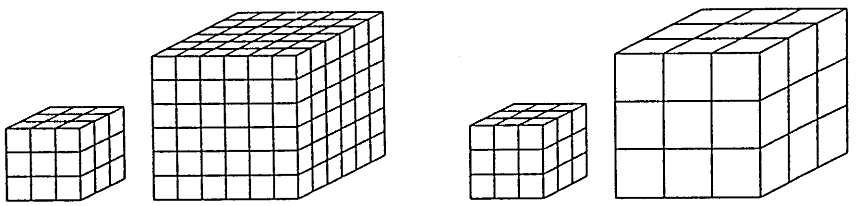

(a)No size effect(pattern A) (b)Similar fragments(pattern B)

Fig.4 Typical cracking pattern of specimen

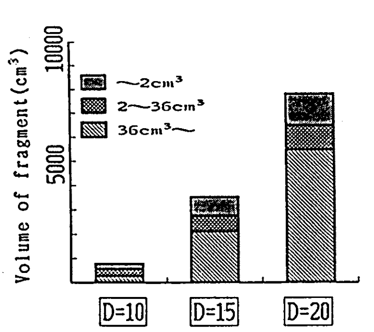

Fig.5 Size distribution of fragments (average)

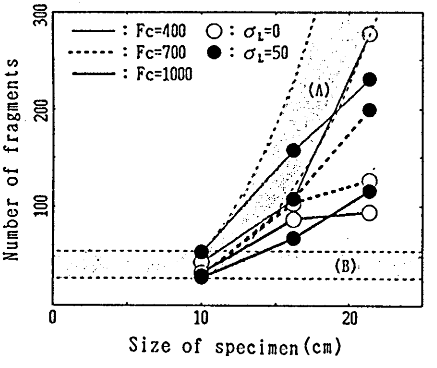

Fig.6 Total number of fragments ($v \geqq 2$ cm^3)

ii)Distribution of fragment

Figures 7(a) and (b) show the measured frequency of medium- and large-sized fragments, respectively. In Fig.7(a), the ordinate represents the relative frequency, where N is the total number of medium-sized fragments. The volume range for medium-sized fragments is classified into 17 ranks from 2 cm^3 to 36 cm^3, at the pitch of Δv=2 cm^3. The median v_m of each rank is given by (2m-1) cm^3, where m is an integer in the range 2 to 18. According to Fig.7(a), relative frequency n/N sharply decreases with increasing fragment volume, regardless of the size of the specimen. This tendency is considered to correspond to typical cracking pattern A in Fig.4, and is also observed in the other sets of Fc and σ_L. The relation as in Fig.7(a) may be represented by Eq.(3) in Table 3.

On the other hand, the range of volume v from V/3 (where, V is the total volume of a specimen) to approximately v=36 cm^3, in the abscissa of Fig.7(b), is divided at the pitch of every half, i.e., at V/6, V/12, ..., from the maximum value V/3. The number of large-sized fragments is almost in a linear relation

Table 3 Numerical equations for number of concrete fragments ($v \geqq 2$ cm^3)

Eq. (2)	$N = a(D-9)+25$ where, $a = -0.9\sqrt{Fc} + 35$ Fc:Compressive strength of concrete(kgf/cm^2) D:Diameter of Specimen (cm) Tenth's position of N is raised.
Eq. (3)	$\frac{n}{N} = \frac{2}{(v_m-1)^2}$ where, v_m=2m−1 m : Integer of 2 to 18 Tenth's position of n is raised.
Eq. (4)	$n = m, \quad v_m = \frac{V}{3} \cdot 2^{-m}$ (m=1, 2, ···) where, $v_m \geqq 36$, V : volume of specimen (cm^3)

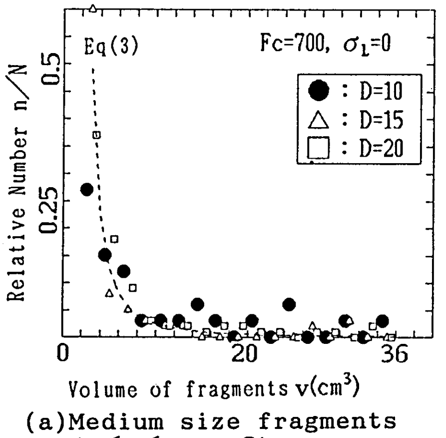

(a)Medium size fragments ($2 \leqq v \leqq 36$ cm^3)

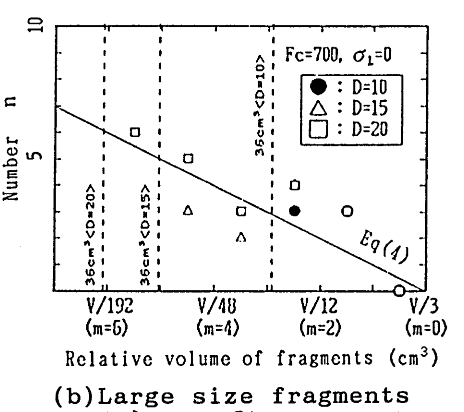

(b)Large size fragments ($v \geqq 36$ cm^3)

Fig.7 Frequency of fragments of various sizes with the relative volume of fragments in the lateral axis, and is given by Eq.(4) in Table 3, regardless of the size of the specimen, concrete strength, or lateral confining pressure. This means the distribution of large-sized fragments corresponds to typical cracking pattern B in Fig.4, which is already predicted in the observation of Photo.1.

3.6 Cracking pattern model

(1)Relation with typical cracking pattern
The cracking patterns of specimen observed in the experiment seem to be between patterns A and B in Fig.4. This fact means that the total energy absorbed over the whole specimen is inevitably influenced by the size of the specimen, assuming that the distribution energy per unit area at cracking is constant, regardless of the size of the specimen.

(2)Cracking pattern model
An ideal cracking pattern for energy dissipation system of compressive concrete may be assumed as in Fig.8, referring to the result from the present experiment. Note that the occupancy ratio of each size of fragment varies with the size of the specimens, as well as with the concrete strength, which is represented by Eq.(2) in Table 3.

(3)Comparison of calculated results with fragments in Photo.1
As an example, the distribution pattern of concrete fragments (assumed to be cubic) is calculated with Eqs.(2) to (4) and shown in Fig.9. The conditions for the present calculation are summarized in Table 4. Here, the total volume of the medium- and large-sized fragments ($v \geqq 2$ cm^3) is assumed to be 80% that of the original specimen, based on the result in Fig.5. All the remaining small-sized fragments ($v \leqq 2$ cm^3), constituting 20% of the total volume, are assumed to be cubes of volume 1 cm^3. Rather similar distributions to those in Photo.1 are obtained, although the total volumes are not necessarily equal to the original ones (within original volume ±10%).

3.7 Dissipation energy per unit area at cracking

The dissipation energy (e) per unit area at cracking is assumed to be given by the following formula:

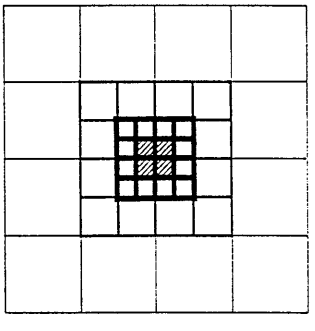

Fig.8 An ideal cracking pattern for energy dissipation system

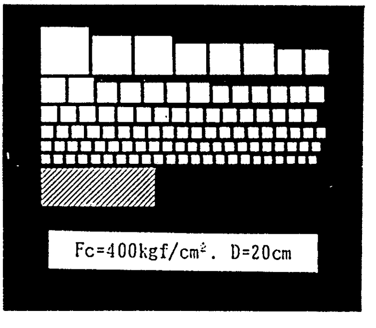

Fig.9 A calculated result of concrete fragments

Table 4 Conditions for present calculation of cracking pattern

1)Shape of fragments: cubes
2)Occupancy ratio of fragments to total volume:
small ($v \leqq 2$ cm^3) 20%
medium ($2 \leqq v \leqq 36$ cm^3) } 80%
large ($v \geqq 36$ cm^3) } (approx.)
3)Frequency of medium and large sizes of fragments:
Eqs.(2) to (4) in Table 3
4)Sizes of small fragments: $v=1$ cm^3

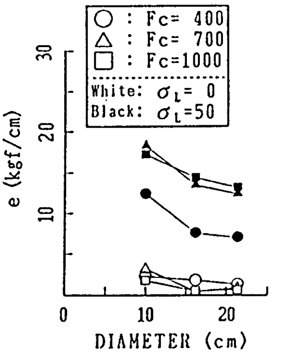

Fig.10
Dissipation energy per unit area of cracked surface

$$e = W_P/A \tag{5}$$

where, W_P: Plastic work by concrete (kgf·cm)

$W_P = \int \sigma_1 d\varepsilon_1$

A: Total area of cracked surfaces (cm^2)

$A = 3\{\Sigma(v^{2/3}) - (\Sigma v)^{2/3}\}$

where, v: Volume of cubic fragment

In Eq.(5), plastic work W_P is taken directly from the uniaxial and triaxial compression test data. The total area of cracked surfaces A is calculated by using the equations in the previous section, under the assumption that all the concrete fragments are cubic.

Figure 10 shows the calculated values of e at $\varepsilon=10\text{x}10^{-3}$ for $\sigma_L=0$ and $\varepsilon=20\text{x}10^{-3}$ for $\sigma_L=50$ series. According to the figure, the values of e for $\sigma_L=50$ kgf/cm^2 series are about 10 times those for $\sigma_L=0$ kgf/cm^2. The values of e tend to decrease with increasing size of specimens. In addition, the value of e for $\sigma_L=0$ series is nearly 1 to 3 kgf/cm, which is estimated to be about 10 times that dissipated per unit area in tensile cracking.

4. Conclusions

1)The effect of specimen size on the deformation behavior of concrete under triaxial compression is more remarkable than that under uniaxial compression (Fig.2).

2)Cracking patterns of the specimens with different sizes are different from each other. Typical cracking patterns are illustrated in Fig.4. The actual patterns were found to be somewhere in-between.

3)The cracking pattern was influenced by the concrete strength, while the effect of lateral confining pressure was scarcely observed (Fig.6).

4)Based on the data-analysis, a model of compressive cracking pattern is proposed. A general idea of the model is illustrated in Fig.8, and an example of the calculated sizes of cubic concrete fragments is shown in Fig.9.

5)The following approximate values were obtained by using Eq.(5) in the calculation of dissipation energy (e) per unit area in compressive cracking (Fig.12):

e = 1 to 3 (kgf/cm) for σ_L=0 kgf/cm^2

e = 7 to 18 (kgf/cm) for σ_L=50 kgf/cm^2

where, the volume of small-sized fragments ($v \leqq 2$ cm^3) was assumed to be the constant value of 1 cm^3.

Conversion units

1 kgf/cm^2=0.098 N/mm^2

1 N/mm^2=1 MPa

5 References

[1]Blanks, R.F. and McNamara, C.C., "Mass concrete tests in large cylinders." J. ACI, 31, 3, 280-303, 1935.

[2]Neville, A.M., "Influence of size of concrete test cubes on mean strength and structural deviation," **Mag. Con. Res.**, 8, 23, 101-110, 1956.

[3]Sangha, C.M. and Dhir, R.K., "Strength and complete stress-strain relationships for concrete tested in uniaxial compression under different test conditions," **Mat. et Const.**, 5, 30, 361-370, 1972.

[4]Tanigawa, Y. and Yamada, K., "Size effect in compressive strength of concrete," **Trans. Arch. Inst. Japan**, 262, 13-21 (in Japanese), 1977.

[5]Sabnis G.M. and Mirza, S.M., "Size effect in model concrete," **Proc. ASCE**, ST, 105, ST6, 1007-1020, 1979.

[6]Shioya, T. and Hasegawa, T., "Size effect of concrete structures," **Conc. J., JCI**, 30, 8, 5-15 (in Japanese), 1992.

[7]Department of the interior cement and concrete investigations, **U.S. Bureau of Reclamation, Boulder Canyon Project, Final Report**, Ⅶ, 4, 1965.

[8]Koike, S. and Hatanaka, S., "Effect of size and slenderness ratio of specimen on stress-strain behavior of confined ultra-high strength concrete," **Trans. JCI**, 14, 369-376, 1992. [9]Koike, S. and Hatanaka, S., "Effect of size and slenderness ratio of specimen on stress-strain curve of confined concrete," **Trans. JCI**, 12, 77-84, 1990.

[10]Hatanaka, S., et al., "Stress strain model for normal and high-strength concrete under triaxial compression," **Trans. JCI**, 13, 125-132, 1991.

[11]Hatanaka, S., Kondo, Y., and Tanigawa, Y., "Effective lateral pressure due to various types of hoops in confined high-strength conc.," **Trans. JCI**, 14, 377-384, 1992.

[12]Kim, J.K. and Eo, S.H., "Size effect in concrete specimens with dissimilar initial cracks," **Mag. Con. Res.**, 42, 153, 233-238, 1990.